PROCEEDINGS OF SCIENCE

Offline secondary vertex reconstruction in the CMS detector

Emily Tsai[a,*] **on behalf of the CMS collaboration**

[a] *Northeastern University,*
360 Huntington Ave, Boston, MA, USA

E-mail: e.tsai@cern.ch

Event reconstruction in particle detectors transforms detector signals into physics objects and, in large particle detectors, generally involves track reconstruction, vertex reconstruction, object reconstruction, and object identification. Vertex reconstruction typically involves two steps: clustering reconstructed tracks into vertex candidates, or seeds, and fitting the vertex candidates to obtain vertex parameters. Secondary vertices are used in the identification, or tagging, of displaced jets originating from b and c quark hadronization, and in the tagging of soft jets with low transverse momenta. Displaced vertices are used in the reconstruction of long-lived particles. These proceedings present an overview of methods used by the CMS experiment for offline secondary and displaced vertex reconstruction during Runs 1 to 3 of the LHC. In the Phase 2 upgrade of the CMS detector for the High-Luminosity LHC operation, changes to the triggering system and track reconstruction will affect the performance of secondary vertex reconstruction, which has not undergone major revision since Run 2. Potential methods aimed at improving the baseline performance in Run 3 and Phase 2 are discussed.

12th Large Hadron Collider Physics Conference (LHCP2024)
3-7 June 2024
Boston, USA

*Speaker

PoS(LHCP2024)236

1. Introduction

The reconstruction of interaction vertices, or vertexing, is an essential step in event reconstruction at collider experiments in high-energy physics. The collision vertex is reconstructed as the primary vertex (PV). Decay vertices are displaced from the PV and are reconstructed as secondary vertices (SV) (which are displaced on the order of mm to a few cm) and displaced vertices (DV) (which are displaced on the order of mm to 100 cm or more). Secondary vertexing allows for the identification of b and c jets for heavy-flavour jet tagging and for tagging soft jets with low transverse momenta. Displaced vertexing allows for the reconstruction of long-lived particles (LLPs), such as beyond the standard model (BSM) particles.

Charged particles from decay vertices deposit hits in a detector that can be reconstructed as tracks. Vertexing is then carried out on these tracks in two steps: finding and fitting. Finding vertices involves spatially clustering charged-particle tracks that share a common point of origin. Fitting a vertex involves computing the position and error of the vertex.

Several methods used for SV and DV reconstruction at the CMS experiment [1, 2] are presented in these proceedings. Additionally, potential improvements to the baseline vertexing performance in the Phase 2 upgrade of the CMS experiment [3] during the High-Luminosity LHC (HL-LHC) era [4] are explored.

2. Run 1 and Run 2

Adaptive vertex fitting (AVF) [5] performs vertex fitting from a given cluster of tracks by minimizing the sum of the weighted squared track significances,

$$M(v) = \sum_{i=1}^{n} w_i \left(\chi_i^2(v)\right), \tag{1}$$

using a Kalman filter with deterministic annealing to avoid local minima. The weight, w_i, for each track is computed based on its compatibility with a vertex candidate, v, as

$$w_i \left(\chi_i^2(v)\right) = \frac{\exp(-\chi_i^2/2T)}{\exp(-\chi_i^2/2T) + \exp(-\chi_c^2/2T)}, \tag{2}$$

where the significance $\chi_i^2(v)$ is the distance from the track to v divided by its uncertainty, and χ_c is the significance for which $w_i = 0.5$. T is a given temperature that starts high and ends low following a determinisic annealing schedule, typically of the form

$$T_i = 1 + r(T_{i-1} - 1), \tag{3}$$

where i refers to the i-th iteration and r is the annealing ratio. The condition $0 < r < 1$ is necessary for convergence. AVF iteratively computes all w_i from an initial vertex position and estimates a vertex position using the weights until convergence. It is robust against outlier tracks, and can be used to fit PVs, SVs, and DVs. Figure 1 shows an example of a fit.

Adaptive vertex reconstruction (AVR) [6] was used for b jet identification in Run 1 [7]. AVR iteratively applies AVF to tracks clustered within jets by first fitting the PV with AVF and removing

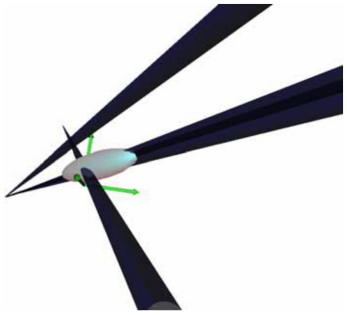

Figure 1: Result of an adaptive vertex fit given four tracks: K^+, K^-, μ^+, and μ^-, where the outlier track is ignored. The black cones represent tracks, and the two middle tracks are very close together. The grey elipses represents the computed vertex position and its error [5].

PV tracks from consideration, then iteratively applying AVF to the remaining unassociated tracks from the previous fit until no more vertices can be fitted. In the second step, deterministic annealing implicitly clusters tracks for fitting. The fit from AVR can be improved by putting a constraint on the initial vertex position.

The inclusive vertex finder (IVF) was adopted for heavy-flavour tagging of b and c jets in Run 2 [7]. From all tracks in an event, it chooses seed tracks using selections on the 3D impact parameter (IP) and 2D IP significance, forms clusters from tracks that are geometrically compatible with the seeds, applies AVF to each cluster, and finally removes duplicate vertices. The IP is the distance between the PV and a track at their points of closest approach (PCA), and the IP significance is the IP divided by its uncertainty. Duplicate vertices are defined as two vertices that either share 70% or more of their tracks, or have a significance of the flight distance between them of less than 2.

Figure 2 shows a comparison of AVR and IVF performance in Run 2 data. Figure 3 shows the performance of IVF in jets where a SV is reconstructed.

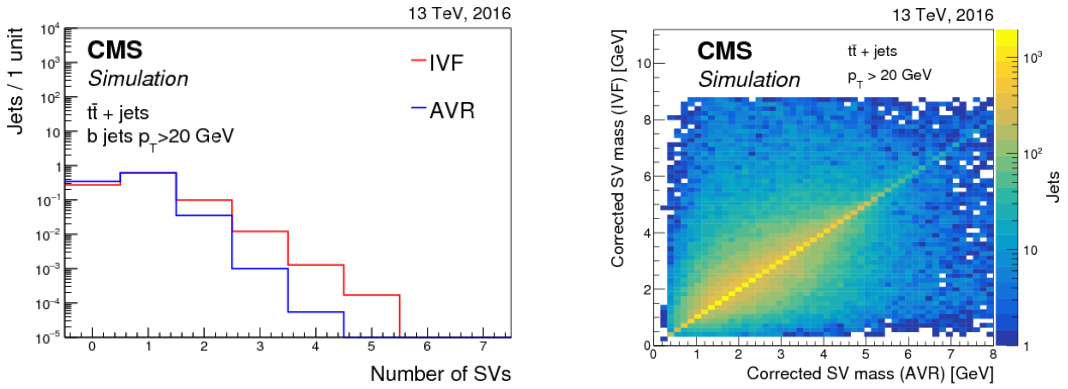

Figure 2: Comparison of Run 2 adaptive vertex reconstruction (AVR) and inclusive vertex finder (IVF) performance. We see that more secondary vertices (SV) are reconstructed with the inclusive IVF approach (left) and the reconstructed SV masses are similar between AVR and IVF (right) [7].

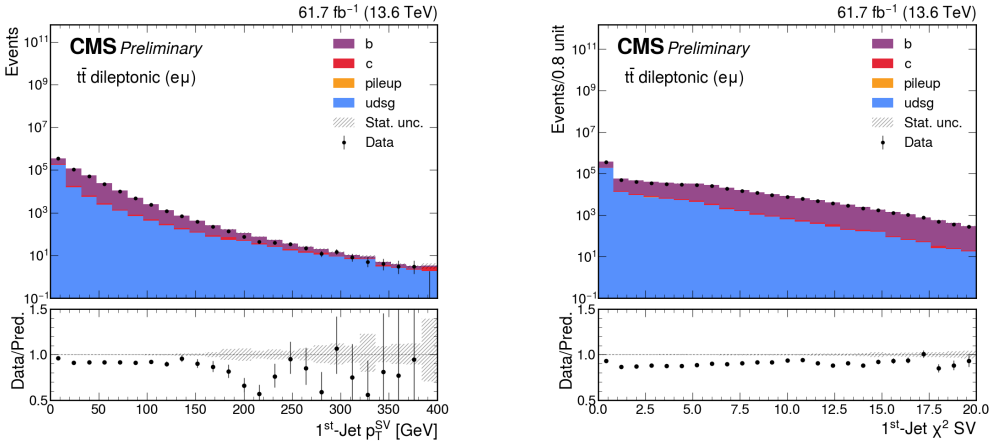

Figure 3: Data to simulation comparison of the secondary vertex (SV) in the first selected jet in each event. Good agreement is observed in the SV p_T (left) and χ^2 (right) distributions [8].

3. Improvements in Run 3 and beyond

A displaced vertexing method that combines AVR and IVF was developed in a search for a long-lived neutral scalar particle, S, that decays to displaced jets. The targeted signal process is shown in Figure 4. The hadronic final states of interest are $S \to b\bar{b}$, $S \to d\bar{d}$, and $S \to \tau\tau$. Current secondary vertexing methods are not expected to capture these displaced vertices well over their full range of possible displacements, thus, this new method was developed. The vertexing method is also sensitive to low-mass hadronically decaying LLPs appearing in many other BSM scenarios.

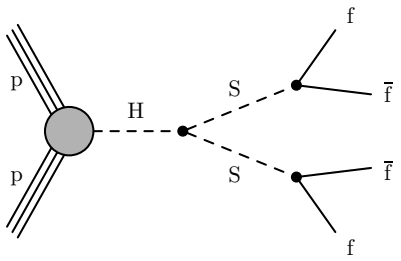

Figure 4: The signal process in the search for an exotic decay of a 125 GeV Higgs boson to two long-lived neutral scalar particles, S, which then decay to displaced jets [9].

The displaced vertexing method uses the following procedure. Given a set of displaced tracks associated to a pair of jets, AVR is first applied directly. Then, seed tracks are found, clusters are formed with geometrically compatible tracks, AVR is applied to each cluster, and finally duplicate vertices are removed. Figure 5 shows the results of the analysis using this displaced vertexing method, which was able to capture displaced vertices well in the $\sim$ 10 cm to $\sim 10^2$ cm range [9].

The introduction of a new subdetector, the MIP timing detector (MTD) [10] for the Phase-2 upgrade, allows for precise measurements of the production time of minimum ionizing particles (MIP). MTD hit clusters, each with an associated position and time, are spatially associated to tracks. The track time at its PCA to the beamline, t_0, is then estimated by taking the difference

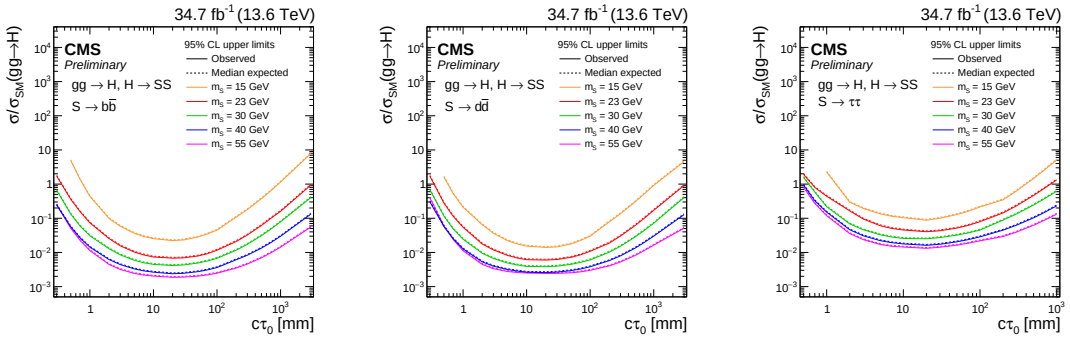

Figure 5: Results from a Run 3 search for an exotic decay to displaced jets using a displaced vertexing method that combines Run 1 and Run 2 methods. The branching ratio (BR) limits are weaker at smaller displacement because only displaced (and not prompt) tracks are used to reconstruct displced vertices. Additionally, BR limits are weaker at larger displacement because track reconstruction efficiency decreases [9].

between the time the track arrived at the MTD and its estimated time-of-flight. PV reconstruction with t_0 included has been studied, where the vertex time is additionally reconstructed using an extension of the deterministic annealing method used to reconstruct PVs. Figure 6 shows how MTD can improve PV reconstruction with t_0 included by separating spatially compatible vertices in time.

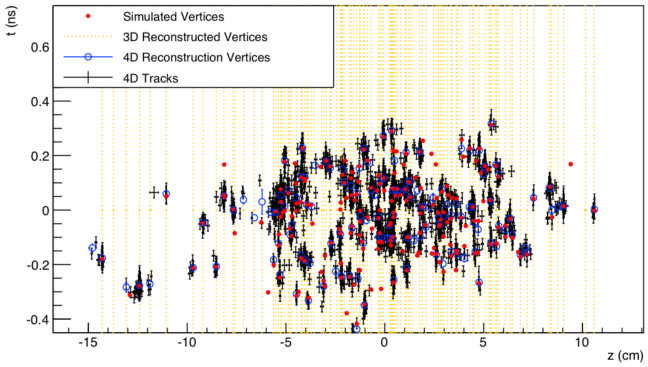

Figure 6: Reconstructed primary vertices including timing information from the MIP timing detector, where spatially compatible vertices are separated in time. This separation is visualized by vertical yellow lines [10].

There are several ways that track timing information can potentially be used to improve secondary vertexing, including: improving track cluster quality in IVF by removing outliers before applying AVF, adding time as an extra fit parameter in AVF, and removing pileup from the secondary vertex collection.

4. Summary

These proceedings presented an overview of secondary and displaced vertex reconstruction in Runs 1 to 3 of the LHC. The secondary vertex reconstruction algorithm used in late Run 2 and in Run 3 is shown to perform better than its predecessor, and the current Run 3 performance shows both good agreement between data and simulation, as well as good sensitivity to displaced vertices. Finally, possible improvements to secondary vertex reconstruction in Phase 2 were outlined.

References

[1] CMS Collaboration, *The CMS experiment at the CERN LHC*, *JINST* **3** (2008) S08004.

[2] CMS Collaboration, *Development of the CMS detector for the CERN LHC Run 3*, *JINST* **19** (2024) P05064.

[3] CMS Collaboration, *Technical Proposal for the Phase-II Upgrade of the CMS Detector*, Tech. Rep. CERN-LHCC-2015-010, CERN, 2015.

[4] HL-LHC Collaboration, *High-Luminosity Large Hadron Collider (HL-LHC): Technical design report*, Tech. Rep. CERN-2020-010, CERN, 2020.

[5] R. Frühwirth, W. Waltenberger, P. Vanlaer, *Adaptive Vertex Fitting*, CMS Note 2007.

[6] W. Waltenberger, *Adaptive Vertex Reconstruction*, CMS Note 2008.

[7] CMS Collaboration, *Identification of heavy-flavour jets with the CMS detector in pp collisions at 13 TeV*, *JINST* **13** (2018) P05011.

[8] CMS Collaboration, *Run 3 commissioning results of heavy-flavor jet tagging at* $\sqrt{s} = 13.6$ *TeV with CMS data using a modern framework for data processing*, CMS Detector Performance Summary 2024.

[9] CMS Collaboration, *Search for low-mass long-lived particles decaying to displaced jets in proton-proton collisions at* $\sqrt{s} = 13.6$ *TeV*, arXiv:2409.10806 (2024).

[10] CMS Collaboration, *A MIP Timing Detector for the CMS Phase-2 Upgrade*, Tech. Rep. CMS-TDR-020, CERN, 2019.

PoS(LHCP2024)236